

# Ultrastretchable, cyclable and recyclable 1- and 2-dimensional conductors based on physically cross-linked thermoplastic elastomer gels

Cite this: *Soft Matter*, 2013, **9**, 7695

Kenneth P. Mineart,<sup>a</sup> Yiliang Lin,<sup>a</sup> Sharvil C. Desai,<sup>a</sup> Arjun S. Krishnan,<sup>†a</sup> Richard J. Spontak<sup>\*abc</sup> and Michael D. Dickey<sup>\*a</sup>

Stretchable conductors maintain electrical conductivity at large strains relative to their rigid counterparts that fail at much lower strains. Here, we demonstrate ultrastretchable conductors that are conductive to at least 600% strain and may be strain-cycled without significant degradation to the mechanical or electrical properties. The conductors consist of a liquid metal alloy injected into microchannels composed of triblock copolymer gels. Rheological measurements identify the temperature window over which these gels may be molded and laminated to form microchannels without collapsing the microscale features. Mechanical measurements identify the gel composition that represents a compromise between minimizing modulus (to allow the polymer to be stretched with ease) and maximizing interfacial adhesion strength at the laminated polymer–polymer interface. The resulting 2D stretchable conductors are notable for their ability to maintain electrical conductivity up to large strains, their mechanical durability, and their ability to be recycled easily with full recovery of the component species.

Received 24th April 2013

Accepted 18th June 2013

DOI: 10.1039/c3sm51136g

[www.rsc.org/softmatter](http://www.rsc.org/softmatter)

## Introduction

Stretchable electronics incorporate electronic functionality into substrates that are deformable, conformal and durable.<sup>1–4</sup> Although common solid metals exhibit electrical conductivities on the order of  $10^7 \text{ S m}^{-1}$  at ambient temperature,<sup>5</sup> their corresponding values of elongation to break are relatively low (typically within a few percent strain).<sup>6</sup> Structuring metal films into corrugated geometries on elastomeric substrates represents one way to increase the elongation of such films.<sup>2</sup> Alternative materials, such as carbon nanotube pastes, conductive inks, and nanowire networks have also been explored to overcome the inherent mechanical limitations of solid metals.<sup>2,7–10</sup> Another attractive materials design exploits the deformability of liquid metals, which also possess high conductivities and are capable of withstanding significantly larger strains while remaining electrically conductive.<sup>11,12</sup> Of particular interest in this study is eutectic gallium indium (EGaIn) with a measured<sup>13</sup> conductivity of  $3.4 \times 10^6 \text{ S m}^{-1}$  at 22 °C. Because alloys of gallium develop a thin solid oxide skin at rest, they can be physically molded into a variety of shapes suitable for use as

antennas, electrodes, sensors, self-healing wires, interconnects, and metamaterials.<sup>11,14–27</sup> Injecting this low-viscosity metal into microchannels fabricated in a polymer matrix affords a facile route by which to define its shape and fabricate structures capable of achieving large strains.<sup>12,28</sup>

Thus far, most studies aimed at marrying the electrical conductivity of liquid metals with the robust mechanical properties of polymers (in particular, elastomers) have focused primarily on using polydimethylsiloxane (PDMS) as the polymer matrix due to its low cost and convenience.<sup>29</sup> The extensibility of PDMS is, however, limited and depends on the PDMS grade and sample preparation protocol employed.<sup>30</sup> For example, Sylgard 184 is one of the most popular polysiloxanes employed for this purpose and fails well below 100% strain. In addition, PDMS is subject to mechanical hysteresis upon strain cycling and cannot be fully recycled due to the covalent cross-links that stabilize the molecular network. The extensibility of conductive PDMS infused with metal can be increased to ~225% through the introduction of a microstructure.<sup>31</sup> Other elastomers can likewise be utilized to increase the elongation of liquid metal conductors encased in a polymer matrix. For instance, melt-extruded hollow fibers composed of a thermoplastic elastomer (TPE) maintain conductivity to 700% strain,<sup>12</sup> but the formation of fibers does not afford the same diversity of in-plane geometries that can be produced lithographically through the use of microfluidics. Alternatively, Ecoflex, a platinum-catalyzed polysiloxane, can be stretched to 900% strain,<sup>17</sup> but fabrication considerations associated with the retention of metal-filled microchannels (e.g., sealing and interfacial bonding) limit the

<sup>a</sup>Department of Chemical & Biomolecular Engineering, North Carolina State University, Raleigh, NC 27695, USA. E-mail: [mddickey@ncsu.edu](mailto:mddickey@ncsu.edu)

<sup>b</sup>Department of Materials Science & Engineering, North Carolina State University, Raleigh, NC 27695, USA

<sup>c</sup>Department of Chemical Engineering, Norwegian University of Science & Technology, N-7491 Trondheim, Norway

<sup>†</sup> Present address: Intel Corporation, Chandler, AZ 85226, USA.

practical extensibility to  $\sim 120\%$  strain. Here, we identify another elastomer system that is not only suitable for defining stretchable microchannels that are both durable and cyclable, but also fully recyclable.

Styrenic TPEs, such as poly[styrene-*b*-(ethylene-*co*-butylene)-*b*-styrene] (SEBS) triblock copolymers, constitute a particularly attractive class of materials for use in this regard. These commercial copolymers are inexpensive, moldable and mechanically robust. They commonly undergo microphase separation so that the endblocks self-assemble into nanoscale domains within a thermodynamically incompatible midblock-rich matrix.<sup>32–34</sup> Because the endblock-rich microdomains are glassy at ambient temperature and a substantial fraction of the rubbery midblocks form bridges between neighboring microdomains,<sup>35</sup> a molecular network that endows the material with considerable elasticity is established. Its mechanical properties can be controlled by adding one<sup>36</sup> or more<sup>37</sup> midblock-selective compounds (*e.g.*, aliphatic-rich oils or hydrogenated tackifying resins in the case of SEBS copolymers) that simultaneously alter the modulus and viscoelastic nature of the system. At low copolymer concentrations (but above the critical gel concentration at which the network first develops<sup>38</sup>), midblock-solvated copolymers behave as physical gels capable of achieving giant strains<sup>39</sup> ( $>2500\%$  in some cases) and are broadly suitable for conventional uses as vibration dampening media, pressure-sensitive adhesives and conductive nanocomposites. These physically cross-linked materials generally exhibit relatively low mechanical hysteresis upon strain cycling, which is critically important for stretchable electronic devices. Selectively solvated triblock copolymers can be molded and welded together into laminate structures to form stretchable microchannels.<sup>40</sup> This fabrication process is nontrivial since two layers of material that are largely liquid must be welded without deforming the micromolded features. Processes designed to weld sheets of solvated copolymer networks together are sensitive to copolymer molecular weight and composition and must be tuned accordingly.

Inspired by the potential applicability of this latter finding,<sup>40</sup> we seek to establish the design rules yielding (i) 1- and 2-dimensional microchannels filled with liquid EGaIn in a midblock-solvated SEBS copolymer (hereafter referred to as a TPE gel, or TPEG) and (ii) ultrastretchable, strain cyclable and fully recyclable wires that remain electrically conductive up to at least 600% strain.

## Experimental

The molecularly symmetric SEBS copolymer employed here (G1654) was manufactured by Kraton Polymers and used as-received. The manufacturer lists the styrenic content of this copolymer as 31 wt%. Size-exclusion chromatography analysis showed the molecular weight and polydispersity to be 144 kDa and 1.04. (In previous studies,<sup>41</sup> the molecular weight characteristics of the copolymer reported by the manufacturer were provided.) For consistency with our previous TPEG studies,<sup>37,42</sup> an aliphatic : alicyclic (70 : 30) mineral oil (Hydrobrite 380) with a molecular weight of  $\sim 500$  Da was obtained from Sonneborn, Inc. and used without further purification. Reagent-grade

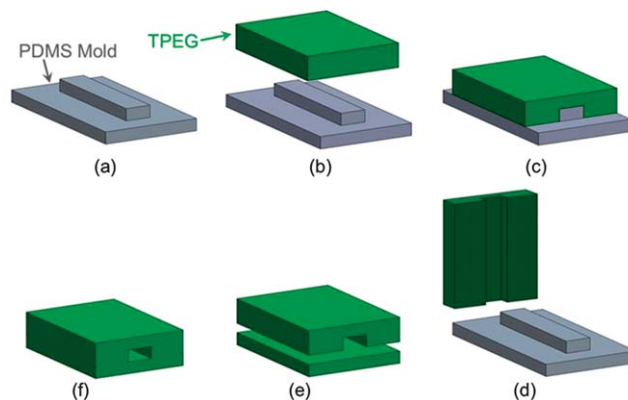


**Fig. 1** Step-by-step procedure by which microchannels are fabricated in TPEGs. A PDMS mold with a desired pattern (a) is first prepared. A TPEG film is melt-pressed onto the mold (b and c) according to the temperature considerations described in the text to leave an imprint of the pattern once the mold is removed (d). The molded TPEG film is melt-pressed with an unmolded TPEG film (e) to yield the desired microchannels (f).

toluene and hydrochloric (HCl) acid were purchased from Sigma-Aldrich and likewise used as-received.

We prepared TPEGs by dissolving the SEBS copolymer and mineral oil in toluene at a concentration of 5 wt% SEBS. Upon stirring for 150 min at ambient temperature, each solution was dried quiescently in a Teflon mold over the course of 72 h, after which time the resultant film was annealed in an oven at  $140\text{ }^{\circ}\text{C}$  for 8 h under vacuum to remove residual solvent and promote nanostructural refinement. All films were hot-pressed into sheets measuring 1.5 mm thick at  $140\text{ }^{\circ}\text{C}$  for an additional 40 min. As schematically depicted in Fig. 1, a PDMS mold subsequently pressed into the film at  $100\text{ }^{\circ}\text{C}$  with minimal pressure generated 1- and 2-dimensional micromolded features. The micromolded film was thermally welded to a flat TPEG film to yield microchannels, which were then filled with liquid EGaIn *via* a syringe.

Dynamic rheology of TPEGs varying in copolymer concentration was performed on a Rheometrics RMS-800 rheometer equipped with parallel plates separated by a 1.0 mm gap. After identifying the linear viscoelastic limit from dynamic strain tests, isochronal temperature sweeps were recorded at a frequency of  $1\text{ rad s}^{-1}$  and a heating rate of  $2\text{ }^{\circ}\text{C min}^{-1}$ . Quasi-static uniaxial tensile and peel (T- or  $180^{\circ}$ ) tests were conducted on an Instron 5943 frame operated at crosshead speeds of 50 and  $60\text{ mm min}^{-1}$ , respectively, at ambient temperature to measure the tensile modulus of each TPEG and the interfacial adhesion between welded TPEG films forming microchanneled laminates. A four-point probe setup was used to measure the conductivity of TPEG/EGaIn composites as a function of strain by attaching electrodes to the composites in close proximity to the grips (which only allowed strains up to 600% before the electrodes induced specimen failure).

## Results and discussion

To develop stretchable conductors containing EGaIn, we first identified the conditions by which to thermally laminate molded and flat TPEG films without deforming the microchannels.

Effective, but minimal, TPEG lamination occurs when the copolymer chains possess sufficient mobility to diffuse across the polymer–polymer interface and create new midblock entanglements. The most effective adhesion occurs by forming mixed micelles across the interface, thereby effectively eliminating the interface and generating a single TPEG capable of achieving maximum elongation without delamination. These conditions must be satisfied while simultaneously preventing excessive chain mobility, which would cause the molded features to collapse or distort, at high temperatures. The rheology-based procedure reported<sup>40</sup> to fabricate stable microchannels in TPEG laminates for microfluidics is extended here for a high-molecular-weight copolymer used to prepare a series of TPEGs varying in copolymer concentration. Rheological measurements identify the temperature range over which TPEG laminate welding can be achieved without negatively impacting the quality of the microchannels. An example of an isochronal temperature sweep of a TPEG containing 25 wt% SEBS is displayed in Fig. 2a for illustrative purposes and identifies two temperatures of interest here.

The first temperature (denoted by an arrow near 130 °C) corresponds to the maximum in the dynamic loss shear modulus ( $G''$ ) and (not shown)  $\tan \delta$ , where  $\delta$  denotes the displacement angle. This temperature, noticeably above the glass transition temperature ( $T_g$ ) of the polystyrene blocks in the SEBS copolymer, is attributed to lattice disordering, which results from endblocks migrating from one molten micelle to another

(a relaxation mechanism commonly referred<sup>43–45</sup> to as endblock hopping) to relieve stresses in the copolymer nanostructure. At temperatures above  $T_g$ , transient dangling endblocks (*i.e.*, endblocks remaining in the incompatible matrix) become more numerous and weaken the network as they diffuse within the matrix in search of new molten micelles to join.

The second temperature (also highlighted by an arrow in Fig. 2a) reveals the order-disorder transition (ODT), at which all long-range nanostructural order is lost and the load-supporting copolymer network fails mechanically as the dynamic storage modulus ( $G'$ ) falls sharply. Since welding oil-rich TPEG films requires that the lattices of the two films be sufficiently soft and flexible to entangle and merge at the molecular level without losing the ability to support an applied load (which would cause micromolded features to collapse), the welding temperature must lie between the lattice dissolution temperature and the ODT. Included in Fig. 2b are both temperatures presented as a function of SEBS concentration. Values of these temperatures depend sensitively on the population of copolymer molecules available to self-organize into a molecular network. As the concentration of SEBS is increased, the width of this process window increases, but laminate welding should be conducted at the lowest temperature defining the window at a given copolymer content. Conversely, the operating window effectively collapses as the critical gel concentration approaches 5 wt% SEBS.

Once the optimal thermal conditions that allow welding are determined, the copolymer concentration that allows substantial uniaxial extension and strong interfacial adhesion must be identified on the basis of mechanical properties. The tensile modulus, shown in Fig. 3a, characterizes the stiffness of each TPEG and scales as (copolymer concentration)<sup>2,36</sup> in quantitative agreement with previously reported results.<sup>42,46</sup> Included for comparison in this figure are data reported by Shankar *et al.*<sup>41</sup> for the same TPEG system up to 30 wt% SEBS. Soft TPEGs possessing low copolymer loading levels can withstand remarkably high strains due to the presence of a loose network with relatively few non-network entanglements. For this reason, we hereafter consider the tensile compliance, given as the reciprocal of the tensile modulus, as a materials design property that should be maximized to enable electronic components that are easy to stretch. Also displayed in Fig. 3a are values of the TPEG laminate adhesion strength, measured in terms of the force required to induce delamination in T-peel tests, as a function of copolymer concentration. The laminate adhesion strength should also be maximized to ensure the microchannels remain intact during deformation. In these tests, both layers of the laminate are identical in terms of composition and molecular weight, and the welding temperature and time employed correspond to 140 °C and 45 min, respectively.

It is not surprising that adhesion strength increases systematically with increasing copolymer content since the probability increases that copolymer chains will span the interface and form entangled midblocks and mixed micelles. The laminate adhesion strength and tensile compliance are cross-plotted in Fig. 3b to identify an optimal SEBS concentration for use in the design of ultrastretchable elastomers featuring microchannels. As seen in Fig. 3b, the discrete

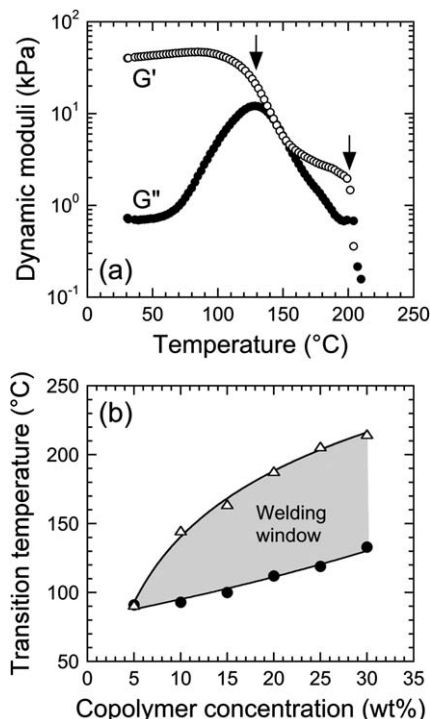


**Fig. 2** In (a), the dynamic shear moduli ( $G'$ ,  $\circ$ ;  $G''$ ,  $\bullet$ ) measured as a function of temperature from a 25/75 w/w SEBS/oil TPEG under isochronal conditions. The arrows identify the upper and lower transition temperatures needed to fabricate microchannels in TPEG laminates. In (b), the upper ( $\Delta$ ) and lower ( $\bullet$ ) transition temperatures comprising the welding window (shaded) for TPEG laminates varying in copolymer concentration.

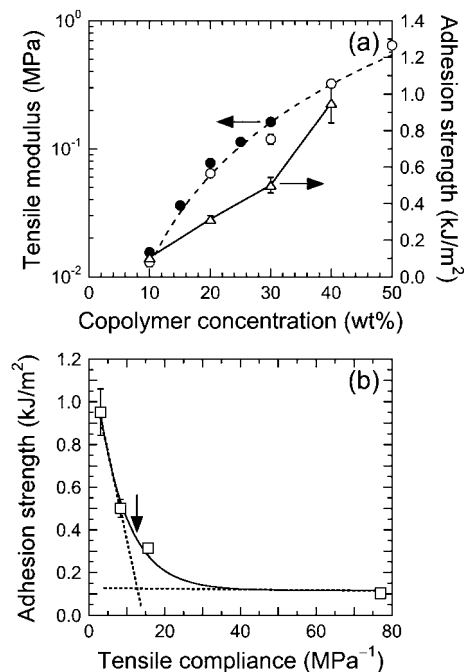


**Fig. 3** In (a), the dependence of tensile modulus (circles: this work,  $\circ$ ; reported results,<sup>40</sup>  $\bullet$ ) and adhesion strength (triangles) on copolymer concentration. The solid line serves to connect the data, whereas the dashed line is a power-law fit to the data. Error bars denote the standard error in the data. In (b), adhesion strength displayed as a function of tensile compliance and fitted to an exponential decay function. The intersection of the dotted tangent lines identifies the cross-over between good adhesion and high compliance and, thus, the composition of the TPEG (20 wt% SEBS) used to fabricate laminates in this study.

experimental data points follow an empirical exponential decay function, which reveals regimes of low and high adhesion strength at high and low compliance levels, respectively. The crossover from high to low adhesion strength is identified by the point of intersection between tangent lines extending from each regime (provided in Fig. 3b). This intersection lies very close to the TPEG containing 20 wt% SEBS, which is soft to the touch, easy to handle and mechanically robust.

By fabricating microchannels in this TPEG (*cf.* Fig. 1) and subsequently injecting EGaIn into the microchannels, we have generated conductive TPEG/EGaIn composites in the form of 1-dimensional wires and 2-dimensional structures, as illustrated by the photographs in Fig. 4a and b, respectively. Due to its inherently low viscosity, the EGaIn wire in Fig. 4a conforms to the shape of the microchannels while the TPEG laminate is strained up to 1000%. Fig. 5a presents the corresponding resistance values ( $R$ , normalized with respect to the initial resistance,  $R_0$ ) of these wires as a function of strain. As expected intuitively, the normalized resistance increases monotonically with increasing strain, and this increase agrees favorably with predictions made solely on the basis of wire geometry (assuming a Poisson's ratio of 0.5). Although the wires could be strained to 1000% by hand before the polymer failed mechanically, the experimental methodology employed for measuring resistance caused the TPEG to fail prematurely just beyond 600% strain. At large strains (*cf.* Fig. 4a), the liquid metal

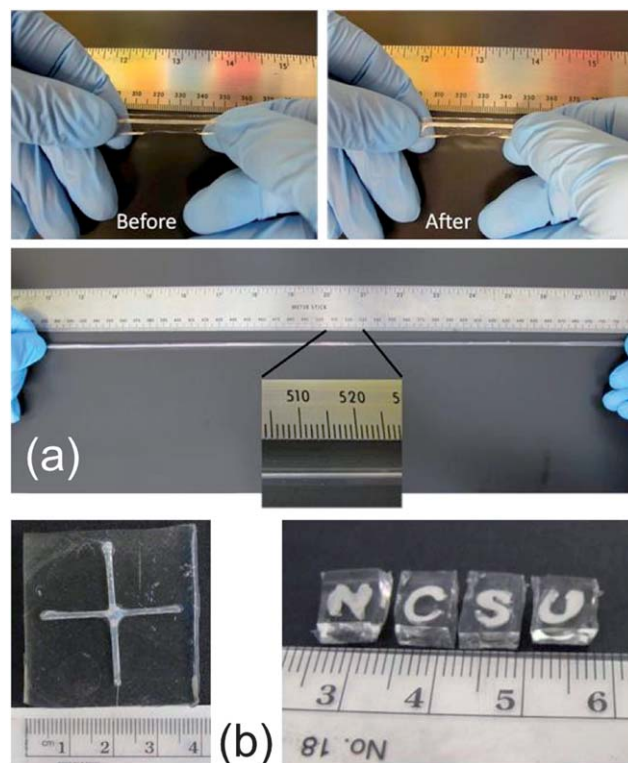


**Fig. 4** In (a), photographs of a TPEG/EGaIn composite before (top left), during (bottom) and after (top right) stretching to 1000% strain to illustrate its ultra-stretchable and elastic nature. In (b), photographs of 2-dimensional arrays that can be achieved by injecting liquid EGaIn into the microchannels fabricated in TPEG laminates.

displays no evidence of physical discontinuity (due to capillary breakup) when observed by eye or under an optical microscope.

An important advantage of TPEGs relative to conventional elastomers is that they tend to exhibit negligible mechanical aging and hysteresis upon strain cycling since their molecular network is a consequence of microphase separation, a thermodynamic process, rather than a kinetically driven reaction process associated with chemical cross-linking. The results displayed in Fig. 5b demonstrate that the TPEG/EGaIn composite can be cycled repeatedly between 0 and 500% strain with less than  $\pm 5\%$  variation in normalized resistance. At larger strain levels (beyond our present measurement capability), we expect that the hysteresis will increase, as evidenced by the mechanical hysteresis loops shown in Fig. 6. The hysteresis energy density ( $E_H$ , the energy within each loop) is included as a function of the maximum strain in the inset of Fig. 6 to provide an indication of the extent to which the hysteresis would likely increase.

Another important feature of TPEGs compared to covalently cross-linked elastomers is that the former, composed of physical (thermoplastic) cross-links, can be reheated or redissolved to disrupt the molecular network and recover a macromolecular liquid. That is, unlike elastomers derived from PDMS or natural rubber, TPEGs can be completely recycled. In an era demanding greater environmental responsibility and material sustainability, this life-cycle consideration is nontrivial. Immersing a



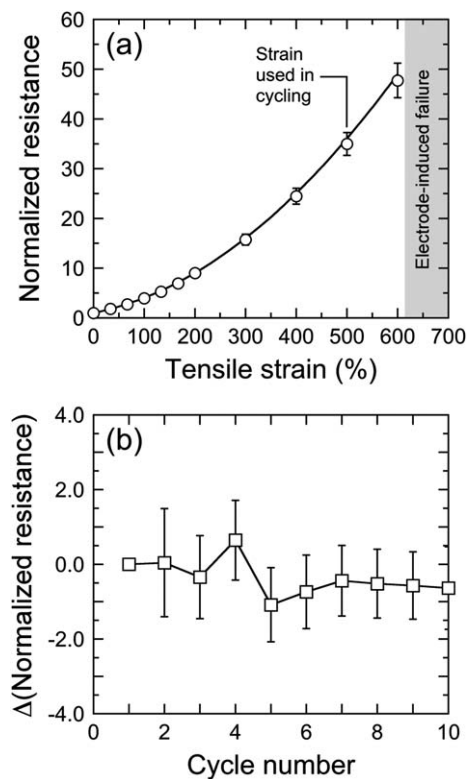


**Fig. 5** Normalized resistance ( $R/R_0$ ) of TPEG/EGaIn composite wires as a function of tensile strain in (a). The change in normalized resistance upon cycling to 500% strain is shown in (b). The theoretical prediction included as the solid line in (a) is determined from  $R = (L/L_0)^2$ , where  $L$  denotes the wire length and  $L_0$  represents the initial length at rest. The solid line in (b) serves to connect the data.

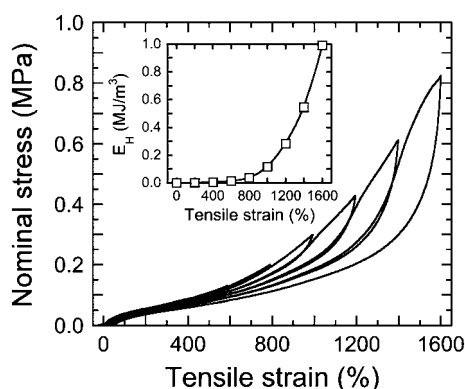


**Fig. 6** Cyclic uniaxial tensile tests with an incremental 200% step strain of the TPEG composed of 20 wt% SEBS at ambient temperature. The inset shows the hysteresis energy density ( $E_H$ ) as a function of the maximum strain in each cycle, and the solid line serves as a guide for the eye.

TPEG/EGaIn composite wire such as the one portrayed in Fig. 7a in a two-phase solvent bath composed of 50/50 w/w toluene/HCl acid promotes concurrent TPEG dissolution and density-driven EGaIn sedimentation as a single bead due to the high surface tension of the metal (the acid removes the oxide skin on the metal surface). This facile separation results in full recovery of all material components.

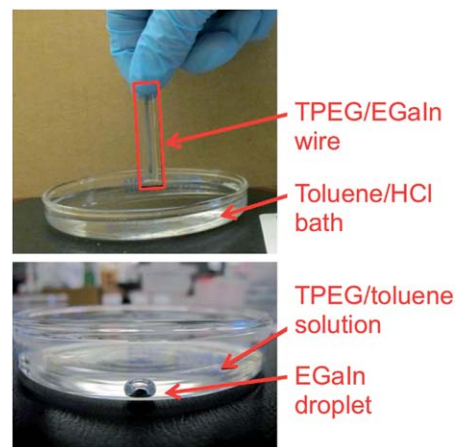


**Fig. 7** A TPEG/EGaIn composite wire prior to recycle (top) and after 10 min of immersion in a mixture of toluene and HCl acid (bottom). The copolymer and oil dissolve completely in the toluene phase, whereas the density of EGaIn and the presence of acid cause the metal to bead up in the bottom of the dish.

## Conclusions

This study establishes that solvated thermoplastic elastomer gels composed of a triblock copolymer swollen with a midblock-selective oil can be micromolded and welded into mechanically robust laminates containing discrete microchannels that can be filled with a liquid metal to produce ultrastretchable conductors. The temperature used for laminate welding lies between the lattice disordering and order-disorder transition temperatures, which are both composition-dependent. A gel consisting of 20 wt% SEBS copolymer represents a trade-off between the tensile compliance and the laminate adhesion strength. Liquid EGaIn injected into 1 or 2-dimensional microchannels generates conductive composites capable of achieving uniaxial strain levels of at least 600% without loss of conductivity, thereby making these materials ideal for use as ultrastretchable and durable conductors. This strain level, which is the maximum measurable but not the maximum achievable, is almost an order of magnitude greater than that of conventional PDMS microchannels filled with alloys of gallium.<sup>29</sup> Repeated strain cycling of these materials to 500% strain has little effect (within  $\pm 5\%$ ) on their electrical and mechanical properties. The conductive substrates can also be flexed, twisted, and deformed easily. In addition to these attractive properties, TPEG/EGaIn composites can be fully separated and their constituents recovered upon dissolution of the copolymer so that new composites can be subsequently fabricated. The ability to pattern ultrastretchable conductors has implications for a number of applications including wires, interconnects, antennas, optical elements, and resonant structures (*e.g.*, metamaterials). The materials described here are particularly attractive for applications that require mechanical durability and physical conformability, or that necessitate large geometric changes to metallic structures.

## Acknowledgements

This work was supported, in part, by Eaton Corporation and the Nonwovens Institute at North Carolina State University. M. D. D.

is grateful for funding from a National Science Foundation CAREER Award (CMMI-0954321) and the NSF Research Triangle MRSEC (DMR-1121107), and R. J. S. acknowledges financial support from the Lars Onsager Professorship at NTNU. We appreciate the assistance provided by Mohammed Mohammed.

## References

- 1 J. A. Rogers, T. Someya and Y. Huang, *Science*, 2010, **327**, 1603.
- 2 J.-H. Ahn and J. H. Je, *J. Phys. D: Appl. Phys.*, 2012, **45**, 103001.
- 3 S. Wagner and S. Bauer, *MRS Bull.*, 2012, **37**, 207.
- 4 J. Zang, S. Ryu, N. Pugno, Q. Wang, Q. Tu, M. J. Buehler and X. Zhao, *Nat. Mater.*, 2013, **12**, 321.
- 5 R. A. Serway, *Principles of Physics*, Saunders College Publishing, Fort Worth, TX, 2nd edn, 1997, p. 602.
- 6 D. Medlin, in *ASM Metals Handbook, Vol. 8: Mechanical Testing & Evaluation*, ed. H. Kuhn and D. Medlin, ASM International, Materials Park, OH, 2000.
- 7 T. Sekitani, Y. Noguchi, K. Hata, T. Fukushima, T. Aida and T. Someya, *Science*, 2008, **321**, 1468.
- 8 K.-Y. Chun, Y. Oh, J. Rho, J.-H. Ahn, Y.-J. Kim, H. R. Choi and S. Baik, *Nat. Nanotechnol.*, 2010, **5**, 853.
- 9 P. Lee, J. Lee, H. Lee, J. Yeo, S. Hong, K. H. Nam, D. Lee, S. S. Lee and S. H. Ko, *Adv. Mater.*, 2012, **24**, 3326.
- 10 F. Xu and Y. Zhu, *Adv. Mater.*, 2012, **24**, 5117.
- 11 H.-J. Kim, C. Son and B. Ziaie, *Appl. Phys. Lett.*, 2008, **92**, 011904.
- 12 S. Zhu, J.-H. So, R. Mays, S. Desai, W. R. Barnes, B. Pourdeyimi and M. D. Dickey, *Adv. Funct. Mater.*, 2013, **23**, 2308.
- 13 D. Zrnic and D. S. Swatik, *J. Less-Common Met.*, 1969, **18**, 67.
- 14 R. C. Chiechi, E. A. Weiss, M. D. Dickey and G. M. Whitesides, *Angew. Chem., Int. Ed.*, 2008, **47**, 142.
- 15 M. D. Dickey, R. C. Chiechi, R. J. Larsen, E. A. Weiss, D. A. Weitz and G. M. Whitesides, *Adv. Funct. Mater.*, 2008, **18**, 1097.
- 16 S. Cheng, A. Rydberg, K. Hjort and Z. Wu, *Appl. Phys. Lett.*, 2009, **94**, 144103.
- 17 M. Kubo, X. Li, C. Kim, M. Hashimoto, B. J. Wiley, D. Ham and G. M. Whitesides, *Adv. Mater.*, 2010, **22**, 2749.
- 18 D. J. Lipomi, B. C.-K. Tee, M. Vosgueritchian and Z. Bao, *Adv. Mater.*, 2011, **23**, 1771.
- 19 C. Majidi, R. Kramer and R. J. Wood, *Smart Mater. Struct.*, 2011, **20**, 105017.
- 20 M. R. Khan, G. J. Hayes, J.-H. So, G. Lazzi and M. D. Dickey, *Appl. Phys. Lett.*, 2011, **99**, 013501.
- 21 J.-H. So and M. D. Dickey, *Lab Chip*, 2011, **11**, 905.
- 22 B. J. Blaiszik, S. L. B. Kramer, M. E. Grady, D. A. McIlroy, J. S. Moore, N. R. Sottos and S. R. White, *Adv. Mater.*, 2012, **24**, 398.
- 23 N. Pekas, Q. Zhang and D. Juncker, *J. Micromech. Microeng.*, 2012, **22**, 097001.
- 24 J. Wang, S. Liu, Z. V. Vardeny and A. Nahata, *Opt. Express*, 2012, **20**, 2346.
- 25 J. Wang, S. Liu and A. Nahata, *Opt. Express*, 2012, **20**, 12119.
- 26 Q. Zhang, Y. Zheng and J. Liu, *Front. Energ.*, 2012, **6**, 311.
- 27 E. Palteau, S. Reece, S. C. Desai, M. E. Smith and M. D. Dickey, *Adv. Mater.*, 2013, **25**, 1589.
- 28 S. Cheng and Z. G. Wu, *Lab Chip*, 2012, **12**, 2782.
- 29 J. H. So, J. Thelen, A. Qusba, G. J. Hayes, G. Lazzi and M. D. Dickey, *Adv. Funct. Mater.*, 2009, **19**, 3632.
- 30 D. S. Lynch and W. Lynch, *Handbook of Silicone Rubber Fabrication*, Van Nostrand Reinhold, New York, 1997.
- 31 J. Park, S. Wang, M. Li, C. Ahn, J. K. Hyun, D. S. Kim, D. K. Kim, J. A. Rogers, Y. Huang and S. Jeon, *Nat. Commun.*, 2012, **3**, 916.
- 32 I. W. Hamley, *The Physics of Block Copolymers*, Oxford University Press, New York, 1998.
- 33 *Thermoplastic Elastomers*, ed. G. Holden, H. R. Kricheldorf and R. P. Quirk, Hanser, Munich, 3rd edn, 2004.
- 34 M. W. Hamersky, S. D. Smith, A. O. Gozen and R. J. Spontak, *Phys. Rev. Lett.*, 2005, **95**, 168306.
- 35 M. W. Matsen and R. B. Thompson, *J. Chem. Phys.*, 1999, **111**, 7139.
- 36 A. S. Krishnan, K. E. Roskov and R. J. Spontak, in *Advanced Nanomaterials*, ed. K. E. Geckeler and H. Nishide, Wiley-VCH, Weinheim, 2010, pp. 791–834.
- 37 A. S. Krishnan and R. J. Spontak, *Soft Matter*, 2012, **8**, 1334.
- 38 M. E. Seitz, W. R. Burghardt, K. T. Faber and K. R. Shull, *Macromolecules*, 2007, **40**, 1218.
- 39 R. Shankar, A. K. Krishnan, T. K. Ghosh and R. J. Spontak, *Macromolecules*, 2008, **41**, 6100.
- 40 A. P. Sudarsan, J. Wang and V. M. Ugaz, *Anal. Chem.*, 2005, **77**, 5167.
- 41 R. Shankar, T. K. Ghosh and R. J. Spontak, *Adv. Mater.*, 2007, **19**, 2218.
- 42 J. H. Laurer, J. F. Mulling, S. A. Khan, R. J. Spontak and R. Bukovnik, *J. Polym. Sci., Part B: Polym. Phys.*, 1998, **36**, 2379.
- 43 H. Yokoyama and E. J. Kramer, *Macromolecules*, 2000, **33**, 954.
- 44 S.-H. Choi, T. P. Lodge and F. S. Bates, *Phys. Rev. Lett.*, 2010, **104**, 047802.
- 45 A. S. Krishnan and R. J. Spontak, *AIP Adv.*, 2011, **1**, 042159.
- 46 D. A. Vega, J. M. Sebastian, Y.-L. Loo and R. A. Register, *J. Polym. Sci., Part B: Polym. Phys.*, 2001, **39**, 2183.